VISUALIZATION OF ACOUSTIC FIELD FORMED BY RADIATION WITH HIGHER-ORDER MODES

Kunitoshi MOTOKI* and Nobuhiro MIKI**

* Faculty of Engineering, Hokkai-Gakuen University
S-26,W-11,Chuo-ku,Sapporo 064,JAPAN *motoki@eli.hokkai-s-u.ac.jp*

** Faculty of Engineering, Hokkaido University
N-13,W-8,Kita-ku,Sapporo 060,JAPAN *miki@hudk.hokudai.ac.jp*

ABSTRACT

Influences of higher-order modes in vocal-tracts upon a speech radiation process are investigated based on acoustic measurement. Though a real vocal-tract has complicated figuration, a uniform rectangular tube was used as a specimen for the theoretical simplicity of wave propagation. The higher-order modes were intentionally excited at one end of the tube, and were radiated from the other end that was mounted flush with a plane baffle surface. Spatial distributions of sound-pressure in the vicinity of the radiation region were measured precisely. The acoustic field is visualized frequency by frequency in terms of amplitude and phase distributions in the radiation space. As the result, the measured distributions of sound-pressure show good agreement with those of the well-known ideal piston model below the first cut-off frequency. Above this frequency, however, quite complicated distributions appear in the radiation space. Distributions of particle trajectories and acoustic intensities are also introduced to visualize the acoustic field. Approximation accuracy of the one-dimensional model of the radiation process is discussed from the viewpoint of the radiated power. These results suggest that in the case of potential excitation of higher-order modes in the vocal-tract, a radiation impedance derived from the piston model should not be used as a boundary condition for the speech radiation process.

1.INTRODUCTION

Radiation characteristics of some lip replicas have been measured in an attempt to establish relationships between lip geometry and its acoustic equivalent (Badin *et al.*,1994). Pelorson *et al.*(1995) has reported theoretical and experimental evaluation on the adequacy of the well-known circular piston model for a speech radiation process from the view point of the lip geometry and higher-order modes. Two or three dimensional acoustic characteristics of vocal-tracts have been also studied by numerical computation methods such as FEM (Lu *et al.*,1993, Matsuzaki *et al.*,1996) or acoustic measurements(Motoki *et al.*,1992) These results have shown the existence of non one-dimensional acoustic field in vocal-tracts even at relatively lower frequencies where plane waves are ordinarily assumed. However, it is still not clear that how the radiation characteristics are influenced by a strong non one-dimensional acoustic field in the vocal-tract, which potentially appears depending on a transverse dimension of the oral cavity.

In this paper, spatial distributions of sound-pressure in a radiation space are measured precisely with different excitation conditions of higher-order modes. Though a real vocal-tract has

complicated figuration, a uniform rectangular tube is used as a specimen for the theoretical simplicity of wave propagation. The higher-order modes are intentionally excited at one end of the tube, and are radiated from the other end that is mounted flush with a plane baffle surface. Spatial distributions of sound-pressure in the vicinity of the radiation region are measured precisely.

As the result, it is well confirmed that the measured distributions of sound-pressure agree with those of the well-known ideal piston model when no propagated higher-order modes are radiated. However, once the first higher-order mode is excited and propagated in the uniform tube, quite complicated sound-pressure distributions appear in the radiation space.

As the relative magnitude and phase of sound-pressure are measured, other acoustic quantities such as particle velocities and acoustic intensities can be computed from the measured sound-pressure data. The radiation acoustic field is also visualized in terms of these quantities. Furthermore, a radiation impedance at the open end of the rectangular tube is also computed from the measured sound-pressure data in order to examine the validity of a one-dimensional representation of the radiation process. These results suggest that in the case of potential excitation of higher-order modes in vocal-tracts, a radiation impedance derived from a simple piston model is not suitable for a boundary condition for the speech radiation process.

2.METHOD

2.1 Experimental setup

A uniform rectangular tube (15mm (= L_z) x 40mm (= L_y), length=600mm) is used as a specimen for the theoretical simplicity of wave propagation. One open end of the tube is mounted flush with a plane baffle surface. A horn driver is used as a sound source, which is connected to the other end of the tube through a connection plate. The horn driver is driven by sinusoidal waves. Sound-pressure distributions in the vicinity of the open end are measured using a probe-microphone installed on a precise mechanical XY-stage. The details of the measurement system are described in Motoki *et al.*(1992). Spatial distributions of amplitude and relative phase are measured frequency by frequency.

The connection plate between the horn driver and the rectangular tube has a small hole (4mm diameter) which is used to change excitation conditions of higher-order modes. The position of the hole is adjustable. When the hole is located on the center of the tube end as illustrated in figure 1(a) where the hole is shown as a filled black circle, only even modes are excited due to the symmetrical shape of tube boundaries. On the other hand, if the hole is located at a corner as illustrated in figure 1(b), odd and even modes are excited.

Cut-off frequencies of some higher-order modes (n_y, n_z), $(n_y, n_z = 0, 1, 2)$ calculated from the sectional dimensions of the rectangular tube are listed in table 1. The lowest cut-off frequency of mode(1,0) is 4.33 kHz at room temperature.

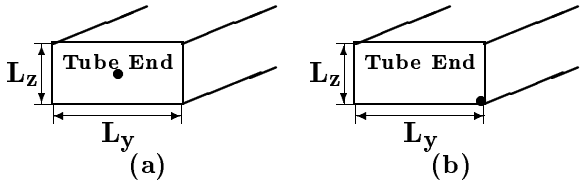

Figure 1 (a) Excitation of even modes.
(b) Excitation of odd and even modes.

Table 1 Cut-off frequencies of higher-order modes. (Unit in [kHz])

$n_z \setminus n_y$	0	1	2
0	0	4.33	8.67
1	11.6	12.3	14.4
2	23.1	23.5	24.7

2.2 Computation of particle velocity

Since amplitude $P(\mathbf{r})$ and phase $\phi(\mathbf{r})$ ($\mathbf{r}$ represents position) distributions of sound-pressure are measured precisely, a particle velocity can be computed from the measured values. Let a complex particle velocity at position $\mathbf{r}$ be $\mathbf{v}(\mathbf{r})$. Sound-pressures and particle velocities are related by Euler's momentum equation as,

$$\nabla(P(\mathbf{r})\, e^{j\phi(\mathbf{r})}) + j\omega\rho\mathbf{v}(\mathbf{r}) = \mathbf{0} \tag{1}$$

where ρ and ω are air density and angular frequency, respectively. Then $\mathbf{v}(\mathbf{r})$ is solved as follows.

$$\mathbf{v}(\mathbf{r}) = \{j\nabla P(\mathbf{r}) - P(\mathbf{r})\nabla\phi(\mathbf{r})\}e^{j\phi(\mathbf{r})}/\omega\rho \tag{2}$$

Spatial gradients of $P(\mathbf{r})$ and $\phi(\mathbf{r})$ are approximated by differences of the measured data.

Multipling $\mathbf{v}(\mathbf{r})$ by the complex time factor $\exp(j\omega t)$ and integrating with respect to time, and then taking the real part, we can obtain an instantaneous particle displacement $\mathbf{d}(\mathbf{r}, t)$.

$$\mathbf{d}(\mathbf{r}, t) = \mathrm{Re}\Big\{ \int \mathbf{v}(\mathbf{r}) e^{j\omega t} dt \Big\} = \mathrm{Re}\Big\{ \frac{\mathbf{v}(\mathbf{r})}{j\omega} e^{j\omega t} \Big\} \tag{3}$$

Then tracing $\mathbf{d}(\mathbf{r}, t)$ through one cycle, we can visualize trajectories of vibrating medium particles.

Once $\mathbf{v}(\mathbf{r})$ is obtained, then a complex acoustic intensity $\mathbf{I}(\mathbf{r})$ can be easily obtained as follows.

$$\mathbf{I}(\mathbf{r}) = \frac{1}{2} P(\mathbf{r}) e^{j\phi(\mathbf{r})} \mathbf{v}^*(\mathbf{r}) \tag{4}$$

Real and imaginary parts of $\mathbf{I}(\mathbf{r})$ are active and reactive intensities, respectively.

3.EXPERIMENTAL RESULTS

Figure 2 shows sound-pressure distributions at 4.5 kHz with different excitation conditions of higher-order modes. The contour intervals are 2.0 dB for amplitude and 10 degrees for phase. Figure 2(a) corresponds to the excitation condition as illustrated in figure 1(a). As the cut-off frequency of the first even mode is higher enough compared to 4.5 kHz, it is justifiably assumed that only plan wave is propagated and radiated. The measured distributions show quite symmetrical field. Figure 3 shows simulated sound-pressure distributions from a well-known ideal piston model at the same frequency of 4.5kHz. The well-known ideal piston model represents a real radiation phenomenon very well when no propagated higher-order modes are excited in the tube.

Figure 2(b) corresponds to the excitation condition as in figure 1(b), where the first odd mode becomes a propagation mode. It is clearly seen that a peculiar point appears outside the rectangular tube where the amplitude of sound-pressure decreases extremely with spatial phase rotation around the center of the amplitude decrease. As the phase becomes discontinuous at the center of the amplitude decreases, sound-pressure becomes absolutely zero at this point. For a real speech production process, this result has an implication that if a recording microphone is located at such point, which may be very close to the lips, the recorded speech might contain spectrum valleys at higher frequencies due to higher-order modes in the vocal-tracts.

Figure 4 shows particle trajectories at 4.5 kHz obtained by the procedure as in equation(3). All elliptical trajectories are drawn in the same size with respect to major axes in order to emphasize the vibrating pattern of the medium. It is seen that while the vibrating pattern in the radiation space is almost one-dimensional for the condition of plane wave propagation, particle trajectories become quite elliptical especially near the absolute zero sound-pressure point when the first higher-order mode is radiated.

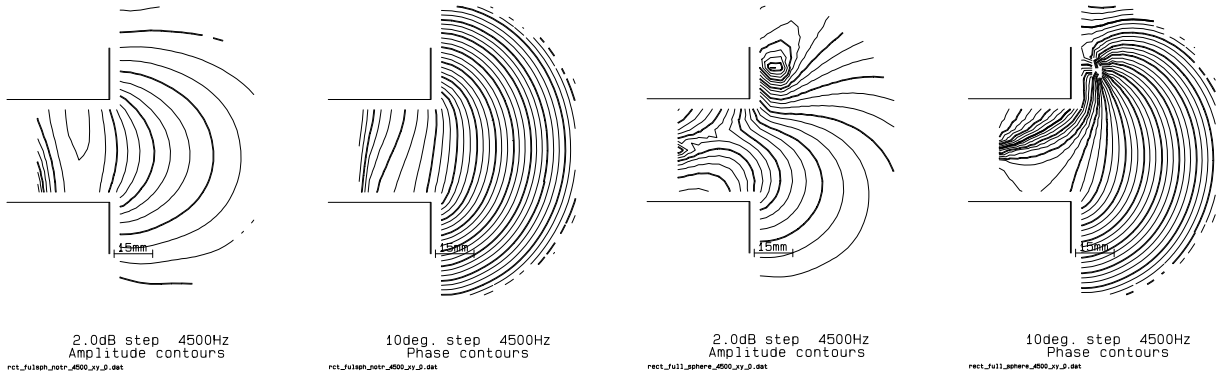

(a)Center excitation. (b)Corner excitation.

Figure 2 Measured sound-pressure distributions at 4.5 kHz.
(a) Plane wave only. (b) Plane wave + first higher-order mode.

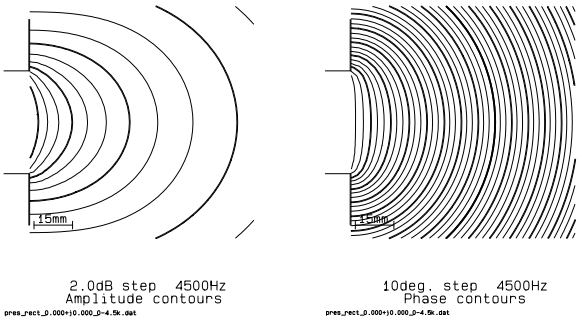

Figure 3 Simulated sound-pressure distributions from an ideal piston model at 4.5 kHz.

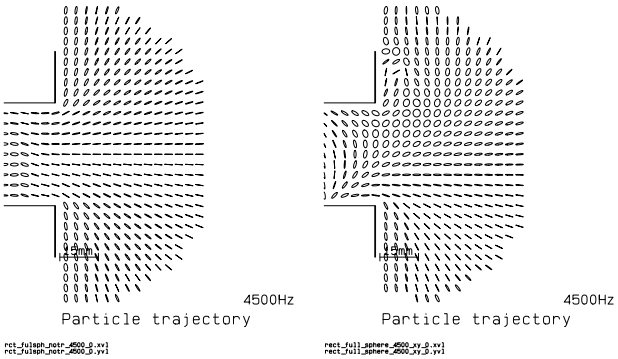

(a)Center excitation (b)Corner excitation.
Figure 4 Particle trajectories at 4.5 kHz.

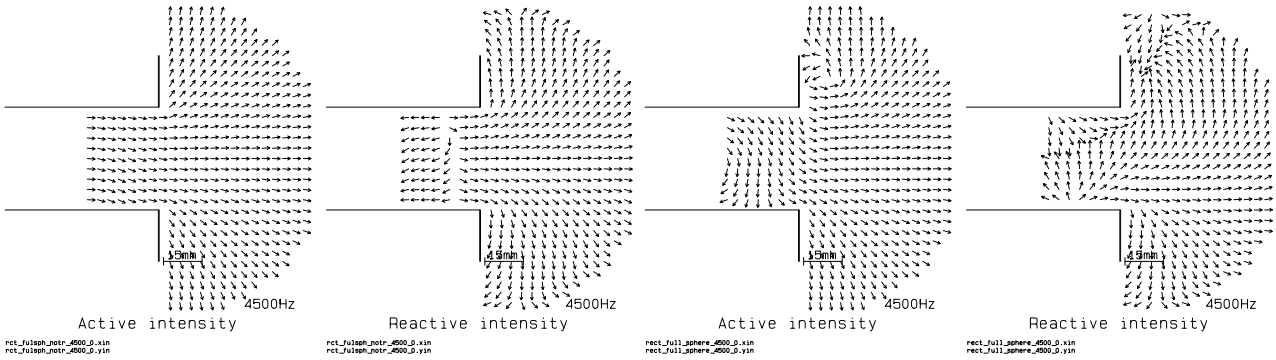

(a)Center excitation. (b)Corner excitation.

Figure 5 Acoustic intensities at 4.5 kHz.
(a) Plane wave only. (b) Plane wave + first higher-order mode.

Figure 5 shows vector maps of active and reactive intensities at 4.5 kHz computed by the procedure as in equation(4). All arrows are drawn in the same size although the magnitudes of intensities vary point by point. In the case of radiation with the first higher-order mode (figure 5(b)), it is clearly seen that the acoustic power is radiated asymmetrically, and active intensity vectors form vortex around the zero sound-pressure point due to the phase rotation of sound-pressure.

4.DISCUSSION

An important parameter characterizing the radiation process is a radiation impedance which is used as a terminal condition of one-dimensional speech production models. Frequency characteristics of the radiation impedance have been studied as a major acoustic problem from the view point of shapes of opening and effects of a baffle surrounding the opening. A circular piston set in a spherical baffle has been considered quite analogous to a real speech radiation process. Thus the radiation impedance for this condition has been widely used in speech production models. In this section, using a direct method we show frequency characteristics of the radiation impedance for the rectangular opening under the condition of higher-order modes propagation in the rectangular tube. And the validity of the one-dimensional model of the radiation process is discussed from the view point of the radiated power.

There are some methods for measuring an unknown acoustic impedance using a uniform tube such as a standing wave method or a transfer function method. These methods are based on assumptions that only plane waves are propagated in the uniform tube and are reflected uniformly by the unknown impedance. In the case of the radiation process in the previous section, we can not apply these methods since higher-order modes are intentionally propagated in the tube.

The radiation impedance Z_L is defined as the ratio of an average of sound-pressure $\bar{p}$ to a volume velocity u over the radiating surface. This can be written as,

$$Z_L = \frac{\bar{p}}{u} = \frac{\frac{1}{A}\int\int_A P(\mathbf{r})e^{j\phi(\mathbf{r})}dS}{\int\int_A v_n(\mathbf{r})dS} \tag{5}$$

where A denotes area of the radiating surface and $v_n(\mathbf{r})$ is a directional component of particle velocity normal to the radiating surface. Since we can compute the particle velocity from equation (2), the volume velocity at the open end of the tube can be directly estimated only from the measured sound-pressure data in the vicinity of the open end. As easily understood, a sensitivity of the probe-microphone and a total gain of the measurement system are cancelled by division in equation (5), which is an important advantage in this measurement.

Figure 6 shows frequency characteristics of Z_L normalized by the characteristic impedance of the uniform tube. Frequency steps are 500 Hz up to 4kHz and 100 Hz up to 9.9 kHz. Theoretical characteristics obtained from the well-known circular piston model with the same radiation area are also drawn in solid lines for the purpose of comparison. The first and second cut-off frequencies are indicated by vertical lines.

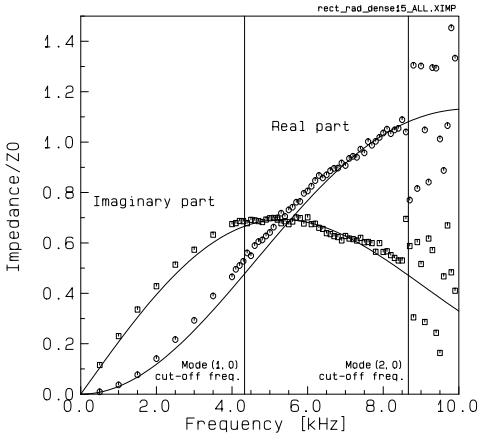

Figure 6 Radiation impedance.

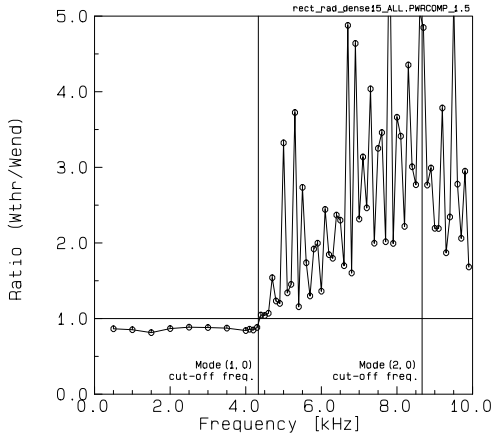

Figure 8 Ratio of effective powers (W_{thr}/W_{end}).

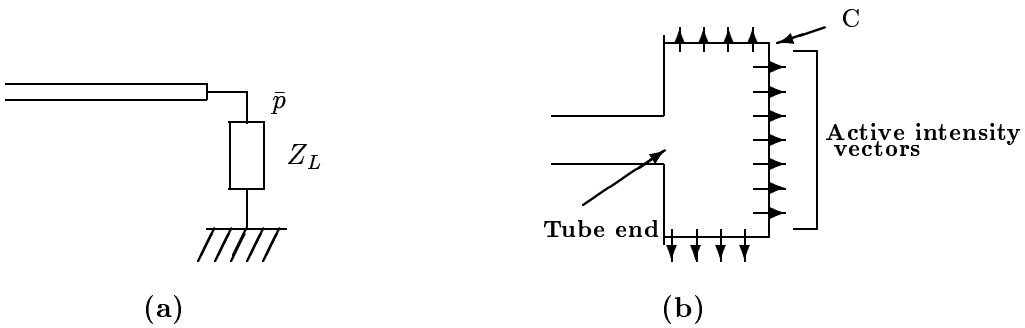

Figure 7 (a) Electrical equivalent representation. (b) Total active intensities on closed surface C.

It can be seen that even at frequencies higher than the first cut-off frequency, both real and imaginary parts of the measured Z_L fairly agree with those of the piston model. For frequencies higher than the second cut-off frequency, the measured Z_L's are quite scattered as the strengths of mode (2,0) relative to plane waves are totally dependent on excitation conditions. The piston model seems valid even at frequencies above the first cut-off frequency. However, this result just reflects a fact that any influence of the first mode (1,0) is cancelled in the averaging procedure in equation (5) since the vibrating pattern of the first odd mode (1,0) is symmetrical with respect to a central plane on the tube axis with a phase difference π. Now, we examine effects of higher-order modes from the view point of radiated power. Let an effective power radiated at the open end of the tube be W_{end}, and an integration of active acoustic intensities over an arbitrary curved or plane surface C that completely encloses the open end be W_{thr}. (See illustration in figure 7.) For one-dimensional representation, W_{end} can be written as,

$$W_{end} = \mathrm{Re}\{|\bar{p}|^2/(2Z_L^*)\} \tag{6}$$

where * means to take a complex conjugate. And W_{thr} can be written as,

$$W_{thr} = \mathrm{Re}\Big\{\int\int_C \frac{1}{2} P(\mathbf{r}) e^{j\phi(\mathbf{r})} (\mathbf{v}^*(\mathbf{r}) \cdot \mathbf{e}_n) dS\Big\} \tag{7}$$

where $\mathbf{e}_n$ is a unit vector normal to C. If the radiation impedance derived from the piston model is valid representation of the real radiation process, then W_{end} should be equal to W_{thr} since the medium is sufficiently assumed to be lossless.

Figure 8 shows the ratio of W_{thr} to W_{end}. W_{thr}'s are obtained on a relatively large vertical plane located 1.5 mm anterior to the open end. Although this plane does not completely enclose the open end, we consider that most of the radiated power is propagated through this plane. While these ratios remain constant around 0.85 below the first cut-off frequency, drastic variation appears above the first cut-off frequency, which implies that Z_L derived from the piston model does not represent real radiation characteristics above the first cut-off frequency.

5.SUMMARY

Distributions of sound-pressure in the near field of the radiation space were measured with different excitation conditions of higher-order modes. Other physical acoustic parameters were also introduced to examine the radiation characteristics. These results suggest that once higher-order modes are excited and propagated in vocal-tracts, the radiation characteristics can not be represented by the lumped radiation impedance derived from the well-known ideal piston model.

Part of this paper has been presented at "The Third ASA and ASJ Joint Meeting", Honolulu,Hawaii.

ACKNOWLEDGEMENT

The authors wish to thank Dr. Pierre Badin (ICP,France) for his valuable suggestions and help in acoustic measurement.

REFERENCES

Badin,P., Motoki,K., Miki,N., Ritterhaus,D., and Lallouache,M.-T. (1994). "Some geometric and acoustic properties of the lip horn," J. Acoust. Soc. Jpn.(E), **15**, 243-253.

Lu,C., Nakai,T., and Suzuki,H. (1993). "Finite element simulation of sound transmission in the vocal tract," J. Acoust. Soc. Jpn.(E), **14**, 63-72.

Matsuzaki,H., Miki,N., and Ogawa,Y.(1996). "FEM analysis of sound wave propagation in the vocal tract with 3-D radiation model," J. Acoust. Soc. Jpn.(E), **17**, 163-166.

Morse,P.M., and Ingard,K.U.(1968). *Theoretical Acoustics*, (McGraw-Hill, New York).

Motoki,K., Miki,N., and Nagai,N.(1992). "Measurement of sound-pressure distribution in replicas of the oral cavity," J. Acoust. Soc. Am., **92**, 2577-2585.

Pelorson,X., Badin,P., Motoki,K., Miki,N., and Plicque,M. (1995). "On the radiation of sound at the lips during speech. Effects of lips geometry and of higher acoustical modes," Proc. ICA95, **4**, 497-500, Trondheim, Norway.